21th International Conference on Renewable Energies and Power Quality (ICREPQ'23)
Madrid (Spain), 24th to 26th May 2023
Renewable Energy and Power Quality Journal (RE&PQJ)
ISSN 2172-038 X, Volume No.21, July 2023

A path planning approach for unmanned solar-powered aerial vehicles

A. Ailon

School of Electrical and Computer Engineering
Ben Gurion University of the Negev
Beer Sheva 8410501 Israel
Phone: +97286461518, e-mail: amit@ee.bgu.ac.il

Abstract. Solar energy is an available high-quality source for the operation of many technological systems that fulfil the needs of human society. Among all the many applications, the use of solar energy in aircraft is extremely challenging, with a lot of potential advantages. The application of solar for flight is one of the promising uses of renewable energy, and in particular the possibility of improving the long endurance requirement in complex missions of unmanned aerial vehicles (UAVs) using solar energy is very attractive. In this context, the article deals with the problem of flight path planning in solar-powered UAVs that fly at a constant altitude. The UAV model incorporates kinematic and dynamic equations where the components of the input vector are the thrust force and the bank angle. Planning the flight path relies here on the flatness property of the system. In fact, his property allows us to plan a flight path without solving non-linear differential equations, and most importantly to link the dynamics of the system, the energy lost and the solar energy absorbed during the flight. Some relevant applications of the approach are discussed, and numerical results are demonstrated.

Key words. Solar energy, UAV control, kinematic & dynamic equations, path planning, differentially flat system.

1. Introduction

Unmanned Aerial Vehicles (UAVs) are used in a variety of missions and a growing number of civil and military applications like surveillance, reconnaissance, and rescue in hostile environments. The aerodynamic characteristics and the operational requirements have forced greater consideration of increasingly intensive and complicated nonlinearity [7], [10] and [13]. The need to increase endurance and to extend flight time motivates researchers and users of UAVs to consider the application of solar energy, which is an available high-quality source of energy [16], to power aircraft in flight. This topic has been studied by many researchers, both in relation to autonomous rotary-wing vehicle [4], [8], and [11], and in relation to fixed-wing UAVs, as for example [5], [6], and [15].

In this research we consider the flight path planning problem for a UAV with fixed wings that flies in a constant altitude from point-to-point in a given time interval. Related problems in different contexts have been discussed in previous publications in the literature. For example, the authors of [12] consider the problem of maximizing the final energy of a solar-powered aircraft relative to time histories of the bank angle and the velocity. The analysis regarding the optimization problem in the last article is based on the kinematic model of the UAV. The approach in [14] is based on the neural network controller, where the control objective is to realize autonomous flight navigation for high-altitude long endurance solar-powered UAVs. The authors of [3] use a nonlinear dynamic optimization approach to calculate energy-optimal trajectories for a solar-powered UAV to achieve longer endurance in high-altitude flight.

This article proposes a new approach to planning a flight path for a UAV whose operation is supported by the solar energy source. The flatness concept [9] in the nonlinear systems theory framework is a useful tool in general, and in vehicle control in particular, see for example [1], and is the basis of the current approach. Given the boundary conditions (initial and target points) and the final time to reach the target, we show that it is possible to calculate a flight path which connects the initial point and the target, and uniquely defines a control law (the vector of the thrust and the bank angle signal) that ensures flight of the aircraft towards the target point along the selected path. In particular, the calculation of the required control law is done algebraically and there is no need to solve non-linear differential equations. The advantages of the approach will be discussed in the article. Especially the present approach establishes practical interactions between the dynamics of the UAV and the models of solar energy absorption and the consumption energy. Examples that demonstrate the analytical results are given later in the article.

2. Modelling

In this study we apply an approximate aircraft model that flies at a constant height [10]. Let T be the thrust, D the drag force, L the lift force, $W=mg$ the aircraft weight (g is the gravitational acceleration), V is the longitudinal velocity with respect to the ground (we assume that the atmosphere is at rest relative to the ground), and ψ,μ are respectively, the heading and the bank angles.

The input vector is given by $F(t)=[T(t),\mu(t)]^T$. To ensure that the aircraft does not reach a stalling speed we require that $V(t)\geq\vartheta>0$ where ϑ is a constant. Then,

$$\begin{aligned} \dot{x}(t) &= V(t)cos\psi(t) \\ \dot{y}(t) &= V(t)sin\psi(t) \\ \dot{\psi}(t) &= gL(t)sin\mu(t)/(WV(t)) \\ \dot{V}(t) &= g\left[T(t)-D(t)\right]/W \end{aligned} \tag{1}$$

where [10] $L=C_L\rho SV^2/2$ and $D=C_D\rho SV^2/2$, C_L is the lift coefficient, C_D is the drag coefficient, S is the wing planform area, and $\rho=\rho(h)$ is the atmosphere density at height h.

The centripetal force during rotation is $C=mv^2/r$ where r is the instantaneous rotation radius with respect to an instantaneous point of rotation, and m is the aircraft mass. We have $\dot{\psi}=V/r$ and therefore $C=mV\dot{\psi}$ or $\dot{\psi}=C/(mV)$. In a constant altitude turn we have $Lcos\mu=mg$, $Lsin\mu=C$ and therefore recalling (1):

$$\begin{aligned} \dot{x}(t) &= V(t)cos\psi(t) \\ \dot{y}(t) &= V(t)sin\psi(t) \\ \dot{\psi}(t) &= gtan\mu(t)/V(t) \\ \dot{V}(t) &= g\left[T(t)-D(t)\right]/W \end{aligned} \tag{2}$$

Next, we will consider the mathematical expressions for energy absorption and energy consumption in flight. The solar cells are installed on the upper side of the wings and collect energy from the sun's rays. Let α,β be the elevation and azimuth of the sun, respectively. Following [12], the incidence angle $\gamma(t)$ of the sun's rays on the solar cells is given by:

$$cos\gamma(t)=cos\mu(t)sin\alpha-sin\mu(t)cos\alpha sin(\beta-\psi(t)) \tag{3}$$

Assume (see [12]) that the sun is fixed in the sky during the process and the power collected by the solar system is

$$P_i(t)=\eta_S P_S Scos\gamma(t) \tag{4}$$

where S is the wings' surface area, η_S is the solar cell efficiency and P_S is the solar spectral density. During the interval $[0,t_f]$ the accumulated energy from the sun is:

$$E_i(t_f)=\int_0^{t_f}\eta_S P_S Scos\gamma(t)dt\,. \tag{5}$$

The estimated power lost is [12]:

$$P_o(t)=T(t)V(t)/\eta_p \tag{6}$$

where η_p is the efficiency coefficient of the propeller.

From here one concludes that at the end of the time interval $[0,t_f]$ the energy loss is given by the following equation:

$$E_o(t_f)=\int_0^{t_f}T(t)V(t)/\eta_p dt\,. \tag{7}$$

Finally, the change in the energy during the process is

$$E_i(t_f)-E_o(t_f)=\int_0^{t_f}(P_i(t)-P_o(t))dt\,. \tag{8}$$

3. The flatness property and its application for solar powered UAVs

The flatness concept [9] is a useful analytical tool in the framework of nonlinear system theory. A nonlinear system $\dot{z}=h(z,u)$ with $z\in R^n$ and input $u\in R^m$ is differentially flat if there exists a flat output vector (which can be seen as a fictitious output) $y_f=p(z,u,\dot{u},\cdots,u^{(r)})\in R^m$ such that the pair $\{z^*,u^*\}$ where $z^*=\varphi(y_f,\dot{y}_f,\cdots,y^{(k)}_f)$ and $u^*=\alpha(y_f,\dot{y}_f,\cdots,y^{(k)}_f)$ satisfies the system equation $\dot{z}=h(z,u)$. The application of the flatness property allows us to describe the system by means of a set of m variables $y_{fi}, i=1,2,\ldots,m$.

In the first step we will examine the significance of the flatness property regarding the system (2). Let $y_f(\cdot)=[x(\cdot),y(\cdot)]^T$ and assume that $x(\cdot),y(\cdot)$ are sufficiently smooth functions. In the current analysis we add a restriction on the function $x(\cdot)$ and impose the condition $\dot{x}(t)\geq\delta>0$ where δ is an arbitrary selected constant. Let ψ be given by $\psi=arctan(\dot{y}/\dot{x})$ and $V(\cdot)$ by $V=\sqrt{\dot{x}^2+\dot{y}^2}$. Then $\dot{\psi}=(\ddot{y}\dot{x}-\ddot{x}\dot{y})/(x^2+y^2)$. We set $L=C_L\rho S(\dot{x}^2+\dot{y}^2)/2$, $D=C_D\rho S(\dot{x}^2+\dot{y}^2)/2$ and $\mu=arctan(\dot{\psi}V/g)=arctan((\ddot{y}\dot{x}-\ddot{x}\dot{y})/(g\sqrt{\dot{x}^2+\dot{y}^2}))$

Finally, observing (2) the thrust is presented by

$$T=\frac{W(\dot{x}\ddot{x}+\dot{y}\ddot{y})}{g\sqrt{(\dot{x}^2+\dot{y}^2)}}+\frac{C_D\rho S(\dot{x}^2+\dot{y}^2)}{2}\,. \tag{9}$$

As we see the selected vector (the flat output) $y_f(t)=[x(t),y(t)]^T$ allows us to establish a chain of computations which can be represented by:

$$y_f(t)\to V(t),\psi(t)\to\mu(t),L(t),D(t)\to T(t) \tag{10}$$

where $F(t)=[T(t),\mu(t)]^T$ generates in (2) the trajectory $\varphi(t)=[y_f^T(t),\psi(t),V(t)]^T=[x(t),y(t),\psi(t),V(t)]^T$.

The control objective is to determine a flight path by means of the flat output and to compute a control law $F(t)=[T(t),\mu(t)]^T$ for which the UAV flies from

$\varphi(0)=[x(0),y(0),\psi(0),V(0)]^T$ to a desired target $\varphi(t_f)=[x(t_f),y(t_f),\psi(t_f),V(t_f)]^T$, and to evaluate the final energy stored in the solar-powered aircraft, i.e.,

$$\{E_i(t_f)-E_o(t_f)\}_{F(\cdot)} \tag{11}$$

subject to the dynamic equation (2), the boundary conditions, and the restriction $V(t)\geq\vartheta>0$ for $t\in[0,t_f]$.

In view of the flatness concept we are interested in calculating the energy balance at the end of the process depending on the selected path $y_f(t)=[x(t),y(t)]^T$ for the solar-powered UAV, i.e., (11) will be replaced by

$$\{E_i(t_f)-E_o(t_f)\}_{(x(\cdot),y(\cdot))} \tag{12}$$

subject to the dynamic equation (2), the boundary conditions, and the restriction $V(t)\geq\vartheta>0$ for $t\in[0,t_f]$.

4. Path planning and energy balance calculation

Let, just for the sake of presentation the flat output $y_f=[x,y]^T$ be given by the functions $p(\cdot),q(\cdot)$:

$$x(t)\doteq p(t),\ y(t)\doteq q(t). \tag{13}$$

We then have

$$\begin{aligned} &p(0)=x(0);\ p(t_f)=x(t_f)\\ &q(0)=y(0);\ q(t_f)=y(t_f) \end{aligned} \tag{14}$$

$$\begin{aligned} &\dot{p}(0)=V(0)cos\psi(0);\ \dot{p}(t_f)=V(t_f)cos\psi(t_f)\\ &\dot{q}(0)=V(0)sin\psi(0);\ \dot{q}(t_f)=V(t_f)sin\psi(t_f) \end{aligned} \tag{15}$$

Given the required conditions $\dot{x}(t)\geq\delta>0;\ V(t)\geq\vartheta>0$ and recalling that $V=\sqrt{\dot{x}^2+\dot{y}^2}$ we set

$$\dot{p}(t)\geq\delta>0;\ \sqrt{\dot{p}^2(t)+\dot{q}^2(t)}\geq\vartheta\geq\delta>0 \tag{16}$$

Next, we consider (3) and note that

$$\begin{aligned} cos\gamma &= cos\mu sin\alpha\\ &+cos\alpha sin\mu(cos\beta sin\psi - sin\beta cos\psi) \end{aligned} \tag{17}$$

Using some trigonometric identities, we have (the conditions $\dot{x}(t)\doteq\dot{p}(t)\geq\delta>0$ ensures that all the terms below are well defined):

$$\begin{aligned} &V=\sqrt{\dot{p}^2+\dot{q}^2}\\ &T=\frac{W(\dot{p}\ddot{p}+\dot{q}\ddot{q})}{g\sqrt{\dot{p}^2+\dot{q}^2}}+\frac{C_D\rho S(\dot{p}^2+\dot{q}^2)}{2}\\ &sin\psi = sin\left(arctan\left(\frac{\dot{q}}{\dot{p}}\right)\right)=\frac{\dot{q}}{\sqrt{\dot{p}^2+\dot{q}^2}}\\ &cos\psi = cos\left(arctan\left(\frac{\dot{q}}{\dot{p}}\right)\right)=\frac{\dot{p}}{\sqrt{\dot{p}^2+\dot{q}^2}} \end{aligned} \tag{18}$$

and

$$\begin{aligned} sin\mu &= sin\left(arctan\left(\frac{\ddot{q}\dot{p}-\dot{q}\ddot{p}}{g\sqrt{\dot{p}^2+\dot{q}^2}}\right)\right)\\ &=\frac{\ddot{q}\dot{p}-\dot{q}\ddot{p}}{\sqrt{g^2\left(\dot{p}^2+\dot{q}^2\right)+\left(\ddot{q}\dot{p}-\dot{q}\ddot{p}\right)^2}}\\ cos\mu &= cos\left(arctan\left(\frac{\ddot{q}\dot{p}-\dot{q}\ddot{p}}{g\sqrt{\dot{p}^2+\dot{q}^2}}\right)\right)\\ &=\frac{g\sqrt{\dot{p}^2+\dot{q}^2}}{\sqrt{g^2\left(\dot{p}^2+\dot{q}^2\right)+\left(\ddot{q}\dot{p}-\dot{q}\ddot{p}\right)^2}} \end{aligned} \tag{19}$$

From (6) and the first two equations in (18) we have

$$P_o=\frac{W(\dot{p}\ddot{p}+\dot{q}\ddot{q})}{g\eta_p}+\frac{C_D\rho S(\dot{p}^2+\dot{q}^2)^{3/2}}{2\eta_p} \tag{20}$$

and using (4) and (17)-(19)

$$\begin{aligned} P_i(t)=\eta_s P_s Sg\Bigg(&\frac{\sqrt{\dot{p}^2+\dot{q}^2}\,sin\alpha}{\sqrt{g^2\left(\dot{p}^2+\dot{q}^2\right)+\left(\ddot{q}\dot{p}-\dot{q}\ddot{p}\right)^2}}+\\ &\frac{\left(\ddot{q}\dot{p}-\dot{q}\ddot{p}\right)cos\alpha}{\sqrt{g^2\left(\dot{p}^2+\dot{q}^2\right)+\left(\ddot{q}\dot{p}-\dot{q}\ddot{p}\right)^2}}\frac{\left(\dot{q}cos\beta-\dot{p}sin\beta\right)}{\sqrt{\dot{p}^2+\dot{q}^2}}\Bigg) \end{aligned} \tag{21}$$

Hence, the expressions in (4)-(8) depend explicitly on the terms in (17)-(21), which are well defined functions of the flat output $y_f(t)=[p(t),q(t)]^T$ and its derivatives.

Example 1. We consider the case where the initial state of the system (2) is (we use the MKS system of units):

$$\begin{aligned}\varphi(0)&=[x(0),y(0),\psi(0),V(0)]^T\\ &=[0,0,-\pi/4,20)]^T\end{aligned}$$

and the control objective is to fly to the final state

$$\begin{aligned}\varphi(t_f)&=[x(t_f),y(t_f),\psi(t_f),V(t_f)]^T\\ &=[4000,2000,\pi/3,40)]^T\end{aligned}$$

where $t_f=350$. We assume $\vartheta=8$ (recall that we must have $V_{min}\geq\vartheta$), the wing area is $S=2$, and the weight is $W=mg=19.6$ $(g=9.8\ and\ m=2)$. Assume that the atmosphere density is $\rho=1.1$ and the propeller efficiency is $\eta_p=0.9$. The solar cell efficiency is $\eta_s=0.25$ and the solar spectral density is $P_S=400$. The drag and the lift coefficients are respectively

$C_D = 0.1$ *and* $C_L = 0.15$. Finally, the elevation and azimuth angles are taken respectively as $\beta = 0, \alpha = \pi/2$.

Firstly, in this case we have using (3) (or equivalently equation (17))

$$\cos\gamma(t) = \cos\mu(t). \tag{22}$$

Next, observing (13) we chose

$$\begin{aligned} p\ (t) &= a_p + b_p t + c_p t^2 + d_p t^3 \\ q(t) &= a_q + b_q t + c_q t^2 + d_q t^3 \end{aligned} \tag{23}$$

To fulfil the boundary conditions, we set the algebraic equations (recall (2) and note the following relations $\dot{p}(t) = V(t)\cos\psi(t), \dot{q}(t) = V(t)\sin\psi(t)$):

$$\begin{aligned} &p(0) = 0; \dot{p}(0) = 14.142 \\ &p(350) = 4000;\ \dot{p}(350) = 20 \\ &q(0) = \ 0; \dot{q}(0) = -14.142 \\ &q(350) = 2000;\ \dot{q}(350) = 34.641 \end{aligned} \tag{24}$$

Clearly (24) is equivalent to the linear algebraic equations $A_i C_i = B_i$ *for* $i = p,q$ where the matrices $A_i \in R^{4\times4}$ are invertible (they depend on the initial and final times), $C_i \in R^4$ are the coefficient vectors and $B_i \in R^4$ are the vectors of the required boundary conditions at $t = 0$ *and* $t = 350$. Finally, t he obtained polynomials $p(t)$ *and* $q(t)$ are given respectively by

$$\begin{aligned} p(t) &= 14.142t - 3.9995\times10^{-2}t^2 + 9.2121\times10^{-5}t^3 \\ q(t) &= -14.142t + 3.0817\times10^{-2}t^2 + 7.4044\times10^{-5}t^3 \end{aligned} \tag{25}$$

The flight path projections along the x *and* y axes are given respectively in Figures 1 and 2, while the flight path projection in the xy-plane is given in Figure 3.

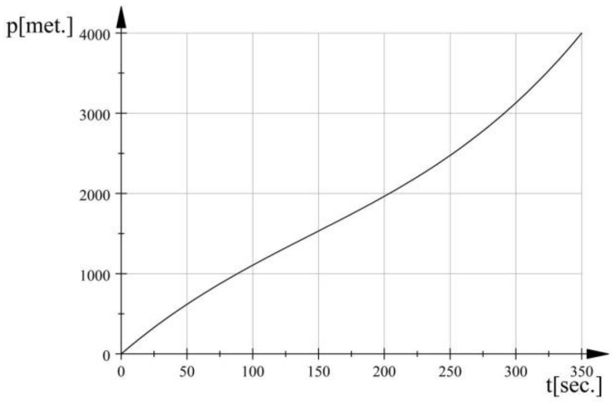

Fig. 1. The flight path projection along x–*axis* in Example 1.

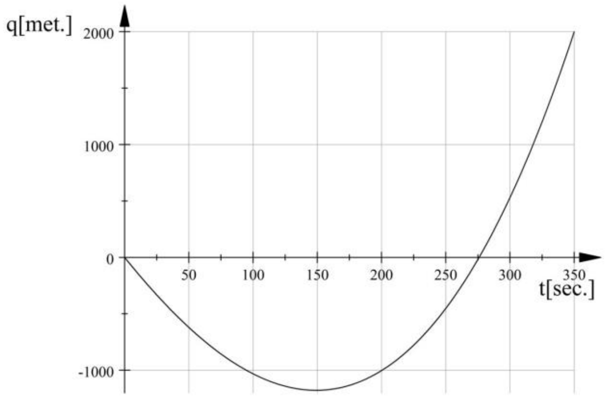

Fig. 2. The flight path projection along $y-axis$ in Example 1.

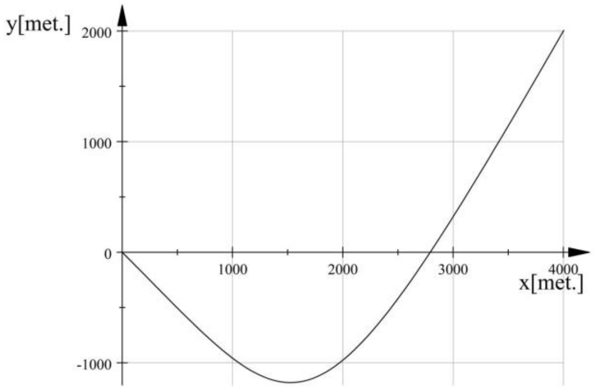

Fig. 3. The flight path projection in $xy-plane$ in Example 1.

From (25) we clearly have:

$$\begin{aligned} \dot{p}(t) &= 14.142 - 0.07999t + 2.7636\times10^{-4}t^2 \\ \ddot{p}(t) &= -0.07999 + 5.\ 5272\times10^{-4}t \\ \dot{q}(t) &= -14.142 + 6.1634\times10^{-2}t + 2.2213\times10^{-4}t^2 \\ \ddot{q}(t) &= 6.1634\times10^{-2} + 4.4426\times10^{-4}t \end{aligned} \tag{26}$$

Applying (26) for $\dot{p}(t), \ddot{p}(t), \dot{q}(t), \ddot{q}(t)$ in (18)-(21) we obtain the time histories of the state variables heading angle and velocity and the thrust and bank angle (input signals), which are shown in Figures 4, 5, 6, 7.

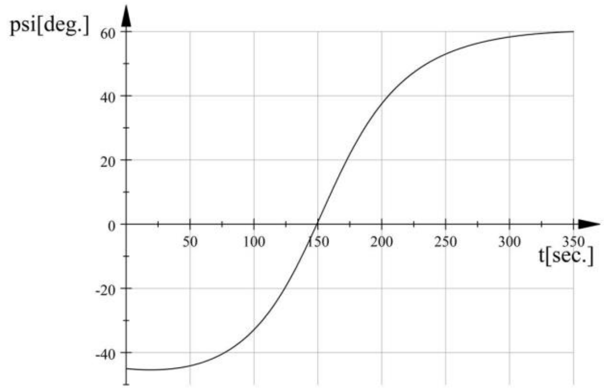

Fig. 4. Time history of the heading $\psi(t)$ in Example 1.

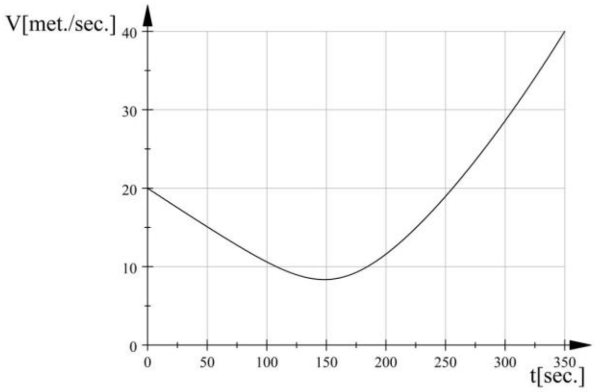

Fig. 5. Time history of the velocity $V(t)$ in Example 1.

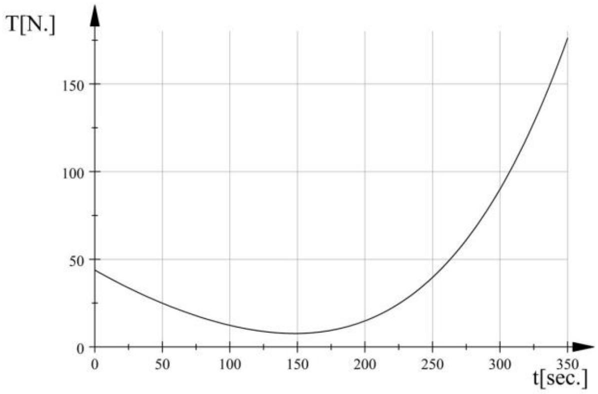

Fig. 6. Time history of the thrust $T(t)$ in Example 1.

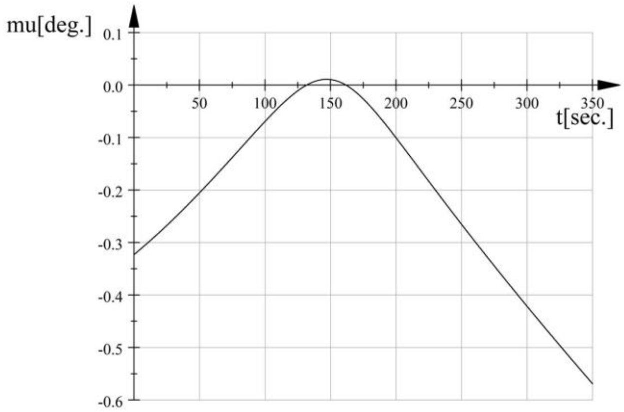

Fig. 7. Time history of the bank angle $\mu(t)$ in Example 1.

Finally, special attention is given to the evolution of the energy balance during the flight from point to point and in particular the final energy state. Observing (4)-(8) and (22) we have in this case

$$E_i(t)-E_o(t)=\int_0^t \left(\eta_S P_S S\cos\mu(\tau)-P_o(\tau)\right)d\tau \qquad (27)$$

where $\mu(\tau)$ and $P_o(\tau)$ are given by (19) and (20). The obtained results are demonstrated in Figure 8.

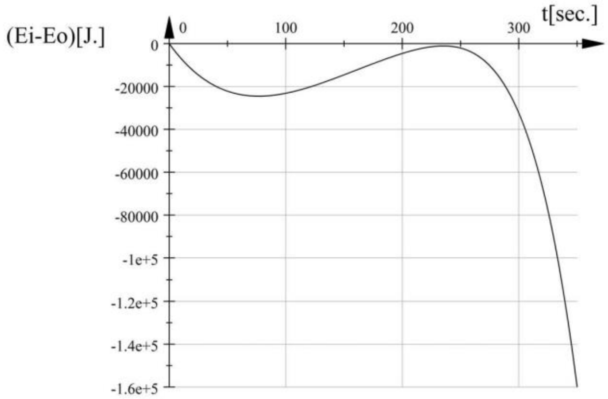

Fig. 8. Time history of the energy balance during flight in Example 1.

At the end of the process, the lost energy is given by $E_i(350)-E_o(350)=-1.5984\times10^5[J.]$. Note that a significant factor in the energy balance is V (in fact, recalling the first two equations in (18) one sees that V raised to the power of 3 in the TV product in (6). Additional attention to this matter is given in the next example.

Example 2. Assume now that the initial state is $\varphi(0)=[x(0),y(0),\psi(0),V(0)]^T=[0,0,-\pi/4,10]^T$ and let the control objective be to fly to the final state

$$\varphi(t_f)=[x(t_f),y(t_f),\psi(t_f),V(t_f)]^T$$
$$=[3000,1500,\pi/3,20)]^T$$

with $t_f=350$. We leave the other parameters as in Example 1. Again, the computations of the relevant polynomial functions $p,\dot{p},\ddot{p},q,\dot{q},\ddot{q}$ (see (23)-(24)) is simple (see Example 1 with the updated boundary conditions). The results are given in Figures 9, 10, and 11. Note that now we have that $E_i(t_f)-E_o(t_f)=E_i(350)-E_o(350)=+33982[J.]$ Also, the condition $V\geq\vartheta=8$ (the stalling speed limit) is still maintained): from Figure 10, at t=100.78[sec.] we get $V_{\min}=8.0317[met./sec.]$.

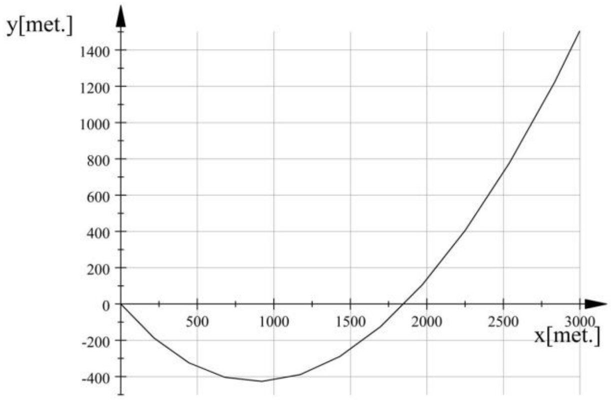

Fig. 9. The flight path projection on the $xy-plane$ in Example 2.

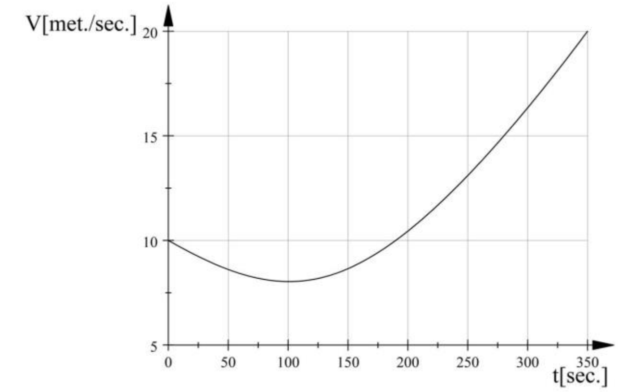

Fig. 10. Time history of the velocity $V(t)$ in Example 2.

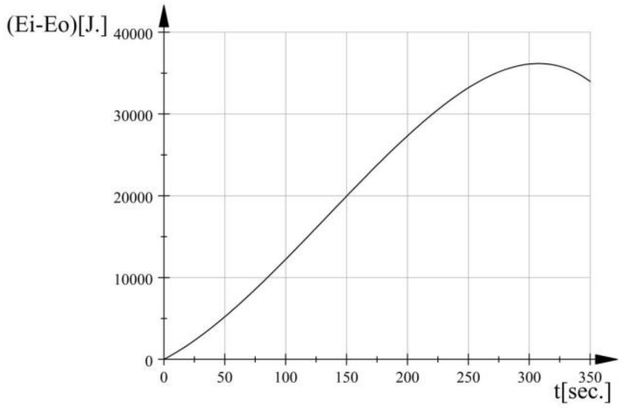

Fig. 8. Time history of the energy balance during flight in Example 2.

Remark. The numerical integral (associated with (8) and (27)), is performed using the midpoint rule (for approximate computations of the area under a simple curve). However, more rigorous research is needed regarding the relevant numerical analysis.

5. Conclusion and future work

Using the concept of flatness from the nonlinear system theory, the paper presents an approach for path planning for a solar-powered UAV that flies in a constant altitude. The presented mathematical procedure is based on algebraic relationships between the flat output and its derivatives and the system state and input variables. These relationships may be useful in evaluating the energy balance with respect to the chosen flight path. It may also be applicable to the search for an optimal (or suboptimal) controller that will ensure an improvement in the energy balance in a given task. In this context the intention is to develop a mathematical procedure that will ensure (as a reference see the equation (8) and (27) above) $\max\{E_i(t_f)-E_o(t_f)\}_{(x(\cdot),y(\cdot))}$, i.e., will maximize the energy balance at the end of the process as a function of the flat output $y_f(\cdot)=[x(\cdot),y(\cdot)]^T$ subject to the differential equation (2) and the system constraints. Another potential advantage is that if during the process it turns out that the preliminary planning is not feasible for energetic reasons, an updated applied route for the UAV can be redefined in real time. It is important to emphasize however that in any case further developments and considerations of the numerical analysis issue is required in order to improve the applied potential of the considered approach.

References

[1] A. Ailon, “Simple stabilizing & tracking controllers for autonomous VTOL aircraft with bounded inputs,” IEEE Transactions on Automatic Control (2010) Vol. 55, pp. 737-743.

[2] J. Anderson, Aircraft Performance and Design, McGraw-Hill, NY (1998).

[3] R.A. Martin, N.S. Gates, A. Ning, and J.D. Hedengren, "Dynamic optimization of high-altitude solar aircraft trajectories under station-keeping constraints," Journal of Guidance, Control, and Dynamics (2018), Vol. 42, pp. 1-15.

[4] R. Bahuguna, R. Sharma, S. Biswas, P. Nandakumar, "Design and analysis of solar quadcopter", Recent Trends in Automation and Automobile Engineering (2020), HBRP Publication, Vol. 3, pp. 1-10.

[5] Y. Chu, C. Ho, Y. Lee, and B. Li, "Development of a solar-powered unmanned aerial vehicle for extended flight endurance", Drones (2021), Vol. 5, pp. 1-19.

[6] N.J. Colella and G.S. Wenneker, "Pathfinder. Developing a solar rechargeable aircraft", IEEE Potentials (1996), Vol. 15, pp. 18-23.

[7] M. V. Cook, Flight Dynamics Principles, Second Edition, Elsevier, Amsterdam, (2007).

[8] K. Daisy, "Design of solar power system for a high endurance quadcopter," available online at: https://extrudesign.com/design-of-solar-powered-quadcopter/ July 9, (2021).

[9] M. Fliess, J. Levine, P. Martin, and P. Rouchon, "Flatness and defect of non-linear systems: introductory theory and examples," International Journal of Control (1995), Vol. 61, pp. 1327-1361.

[10] D. G. Hull, Fundamentals of Airplane Flight Mechanics, Springer-Verlag, Berlin Heidelberg (2007).

[11] N. Kingry, L. Towers, Y.-C. Liu, Y. Zu, Y. Wang, B. Staheli, Y. Katagiri, S.l Cook, and R.Dai, "Design, Modeling and Control of a Solar-Powered Quadcopter" Proceedings of the IEEE International Conference on Robotics and Automation (ICRA), Brisbane, Australia (2018).

[12] A.T. Klesh and P.T. Kabamba, "Energy-Optimal path planning for solar-powered aircraft in level flight," Proceedings of the AIAA Guidance, Navigation and Control Conference, South Carolina, USA (2007).

[13] B. L. Stevens and F. L. Lewis, Aircraft and Simulation, John Wiley & Sons, Inc., Canada (1992).

[14] W. Ni, W. Di, and X. Ma, "Energy-optimal flight strategy for solar-powered aircraft using reinforcement learning with discrete actions" IEEE Access (2016), Vol. 4, pp. 1-22.

[15] K.C. Reinhardt, T.R. Lamp, J.W. Geis, A.J. Colozza, "Solar-powered unmanned aerial vehicles," Proceedings of the Intersociety Conf. on Energy Conversion Engineering (IECEC), Washington, DC, USA, (1996).

[16] W.B. Stine and M. Geyer, Power From The Sun, Power From The Sun.net, www.powerfromthesun.net, (2001).